Journal of Geochemical Exploration 278 (2025) 107832

Contents lists available at ScienceDirect

Journal of Geochemical Exploration

journal homepage: www.elsevier.com/locate/gexplo

The Anthropigene: a new approach in environmental geochemistry to discriminate anomalies from natural background

Lucia Rita Pacifico [a], Francesco Carotenuto [a], Annalise Guarino [a], Antonio Iannone [a], Domenico Cicchella [b], Stefano Albanese [a,*]

[a] Department of Earth, Environmental and Resources Sciences, University of Naples Federico II, 80126 Naples, Italy
[b] Department of Science and Technology, University of Sannio, 82100 Benevento, Italy

ARTICLE INFO

Keywords:
Geochemical gene
Anthropogenic contamination
Anomalies
Geochemical background
Topsoil

ABSTRACT

Assessing the geochemical background is critical for addressing soil contamination, particularly in regions with complex interactions between the natural geological context and anthropic activities. Traditional methods for distinguishing geochemical backgrounds from anthropogenic anomalies often struggle to account for overlapping signals in such areas, leading to limitations in accurately identifying contamination sources. This study introduces the "anthropigene" method, an adaptation of the "geochemical gene" method initially developed for mining applications in the environmental context. By classifying geochemical indicators ("genes") associated with urban and agricultural contamination, the anthropigene provides a robust framework for distinguishing anthropogenic anomalies from natural geochemical signals. Applied to approximately 3000 topsoil samples from the Campania region in Italy, the method allowed the determination of multivariate geochemical patterns linked to urban and agricultural sources of contamination. Samples considered contaminated were eliminated from the original dataset, and the remaining data were used to assess geochemical backgrounds.

Results showed that the background values determined through the proposed approach significantly differed from those generated by applying Italian guidelines; they are also generally more conservative if used as a reference for a tier-one human health risk assessment and environmental restoration. Using the proposed method could have favorable practical implications for unveiling the presence of large-scale diffuse contamination processes that could be easily mistaken for natural enrichments due to their spatial extension.

The method certainly has wide margins for improvement, and future studies will focus on identifying specific indicators of anthropic processes not considered in this paper and improving the techniques for estimating background values at a regional scale.

1. Introduction

In recent decades, environmental geochemistry has emerged as a critical discipline for understanding and managing natural ecosystems and mineral resources. It plays a pivotal role in ensuring the sustainable extraction of resources by minimizing environmental impacts, such as those caused by mining activities, soil degradation, and water contamination through the mobilization of metals (Adriano, 2001). Moreover, environmental geochemistry provides essential methodologies for addressing global environmental challenges, including pollution remediation and climate change mitigation, by elucidating the chemical processes that govern the transport and transformation of contaminants in natural systems (Alloway, 2012).

One of the key objectives in this field is to differentiate geochemical background levels, representing the natural concentrations of chemical elements within specific geological contexts, from anomalies caused by natural processes or human activities. Estimating reliable natural background concentrations is fundamental for distinguishing natural variations from anthropogenic impacts. In mining, such estimations help locate concealed mineral deposits and optimize extraction, while in environmental monitoring, they enable the detection of contamination and the assessment of its effects on ecosystems. Over the years, various methodologies have been developed to accurately separate natural and anthropogenic contributions in environmental media, ranging from univariate and multivariate statistical approaches (Matschullat et al., 2000; Reimann et al., 2005; Négrel et al., 2019) to fractal methods

* Corresponding author.
E-mail address: stefano.albanese@unina.it (S. Albanese).

https://doi.org/10.1016/j.gexplo.2025.107832
Received 6 March 2025; Received in revised form 18 May 2025; Accepted 4 June 2025
Available online 6 June 2025
0375-6742/© 2025 The Authors. Published by Elsevier B.V. This is an open access article under the CC BY license (http://creativecommons.org/licenses/by/4.0/).

(Cheng et al., 1994; Albanese et al., 2007; Zuo and Wang, 2016) and compositional data analysis (CoDA) (Pawlowsky-Glahn and Egozcue, 2006; Reimann et al., 2012).

The "geochemical gene" concept introduced by Yan et al. (Yan et al., 2018) recently provided a novel framework for interpreting geochemical anomalies. This method focuses on stable elemental signatures akin to genetic inheritance and has primarily been applied in mineral exploration and geosciences. Geochemical genes are classified as lithogenic, reflecting the geological characteristics of a region, or metallogenic, associated with mineral deposits. Lithogenic genes use immobile elements as tracers of geological processes, establishing stable geochemical codes that persist under weathering conditions (Yan et al., 2018; Wu et al., 2021). Subsequent studies expanded this approach, introducing metallogenic genes to trace elements such as gold, tungsten, and rare earth elements, demonstrating its utility across various fields, including archaeology and forensic investigations (Gong et al., 2020; Li et al., 2019).

Based on these premises, to expand this approach to the environmental context, we propose here the anthropigene method, an adaptation of the original concept (Yan et al., 2018) which aims at distinguishing geochemical anomalies proceeding from anthropic sources of contamination from the natural fingerprint associated with geology (geochemical background). The proposed approach uses immobile elements to define natural geochemical conditions and indicator elements to identify anthropogenic inputs. By constructing spectral lines and calculating similarity percentages (Gong et al., 2020) relative to an ideal background gene, representative of uncontaminated soil conditions, the method provides a sound solution for identifying and quantifying contamination from urban and agricultural sources. The anthropigene approach provides an advancement in geochemical data analysis by addressing the inherent limitations of traditional methods, such as the potential overestimation of baseline levels due to the inclusion of anthropogenically influenced samples. Unlike conventional statistical approaches, which primarily rely on outlier removal and statistical averages, the method utilizes normalized values and genetic similarity to isolate anthropogenic influences.

In this study, we apply the anthropigene method to approximately 3000 topsoil samples (collected across the Campania region in southern Italy) to distinguish between urban and agricultural sources of contamination, estimate natural geochemical background (baselines, in case of elements featured by a historical diffuse anthropogenic input) following anomaly detection and separation, and compare the results with those eventually provided by "traditional" methods.

2. Study area

The Campania region, located along the Tyrrhenian margin of southern Italy, covers an area of approximately 13,590 km^2 and is one of the most densely populated regions in the country. The geological setting of Campania is complex, composed of volcanic lithotypes (both rocks and loose materials from fall-out), carbonate rocks, siliciclastic deposits, and alluvial sediments (Fig. 1). The eastern sector features the Apennine mountains, a fold and thrust belt system formed during the Miocene, consisting of Mesozoic sedimentary units such as dolostone, limestone, siliceous schists, and terrigenous sediments (Steckler et al., 2008; Pierantoni et al., 2020). The western sector encompasses a Plio-Pleistocene graben, formed due to extensional forces associated with the Apennine chain's formation, filled with siliciclastic, carbonate, and evaporitic sediments, and correlating with the present Campania and Sele plains (Vitale and Ciarcia, 2018). The region's volcanic activity, linked to the Roman Comagmatic Province, extends from 600 ka BP to the present and is evidenced by four major volcanic complexes: Mt. Roccamonfina, Mt. Somma-Vesuvius, Phlegraean Fields, and Ischia Island. Potassic to ultrapotassic rocks are the prominent products of the Campania volcanism, and pyroclastic deposits cover significant portions of the region, including most of the Apennine reliefs and a limited portion of the inner territory (De Vivo et al., 2020; Peccerillo, 2005; Peccerillo, 2017).

Campania's fertile volcanic soils, combined with a favorable climate, result in exceptional agricultural productivity. The region is a major agricultural center in Italy, producing a wide range of crops, including wheat, cereals, potatoes, tomatoes, and fruits such as chestnuts, olives, grapes, and citrus (Albanese et al., 2007). The diverse mineralogical composition of the soils contributes to these agricultural products'

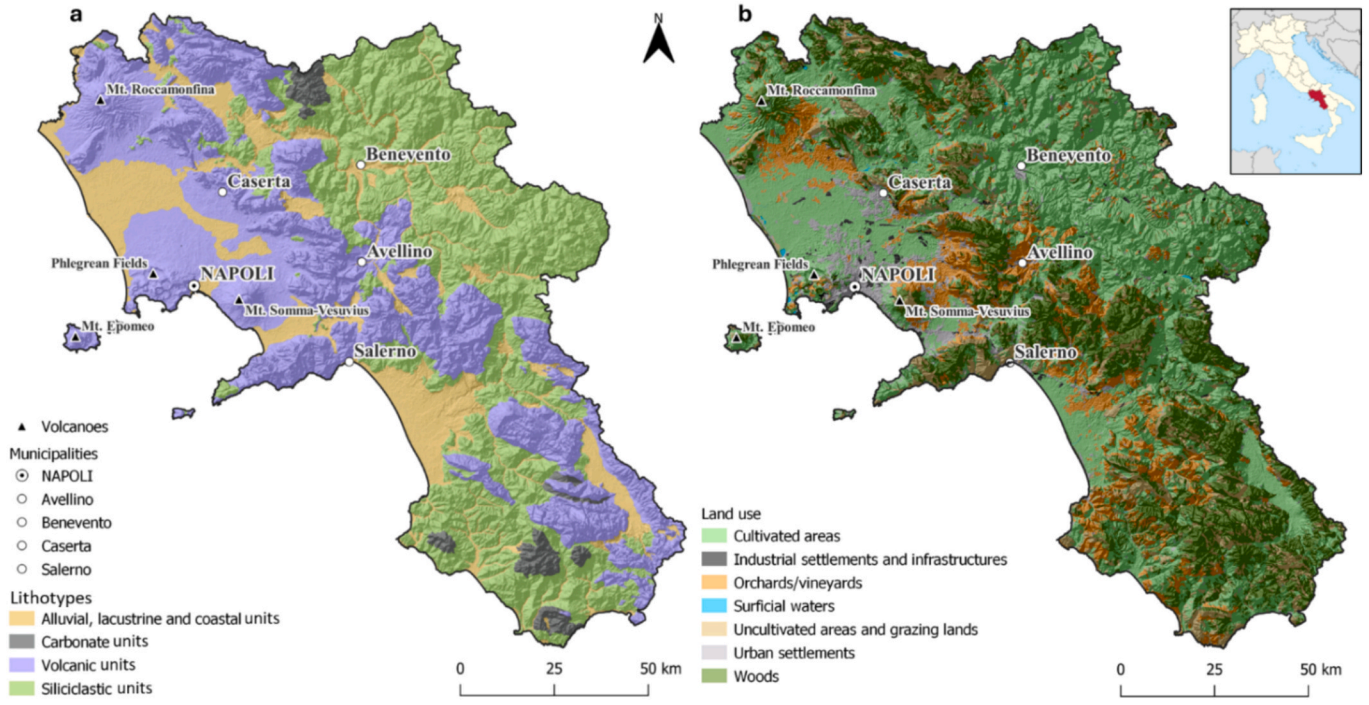

Fig. 1. a) Simplified geological map of Campania region (modified after Guarino et al.2022); b) Land use map (modified after Corine Land Cover, 2018).

unique flavors and nutritional properties (Verdi et al., 2018).

Major urban areas, including Napoli, Benevento, Caserta, and Avellino, are strategically located in the coastal plains and inland regions, fostering both industrial and agricultural activities (Fig. 1b). Industrial zones in Campania are typically situated near urban centers or accessible flat areas, enhancing the synergy between the industrial and agricultural sectors. This proximity contributes to significant urban pollution, particularly pronounced in regions with strong industrial and agricultural economies like Campania. Such pollution primarily arises from emissions related to industrial activities and vehicular traffic. These sources lead to soil contamination, especially with PTEs like Pb, Cu, and Zn (De Vivo et al., 2021; ARPAC, Agenzia Regionale per la Protezione dell'Ambiente Campania, 2021). Furthermore, industrial emissions—including those from coal combustion—combined with the intensive use of pesticides and fertilizers in agriculture exacerbate nutrient imbalances in the soil, resulting in long-term environmental degradation (SNPA, Sistema Nazionale per la Protezione dell'Ambiente, 2023).

3. Materials and methods

3.1. Data

In this study, we analyzed 3751 topsoil samples (collected from a depth of 0–15 cm) covering the entire regional area, with higher sampling density in urbanized zones and lower density in rural areas. The samples were collected up to 2017 as part of the research activities conducted by the Environmental Geochemistry Working Group at the Department of Earth, Environmental and Resource Sciences (DiSTAR) of the University of Naples Federico II (Buccianti et al., 2015; De Vivo et al., 2016; Minolfi et al., 2018; Guarino et al., 2022). Although the samples were gathered over five years, the preparation and analysis methods remained consistent. The soil samples underwent accurate preparation at the DiSTAR Environmental Geochemistry laboratory, which included drying at temperatures below 37 °C to minimize Hg volatilization. Each sample (approx. 30 g, < 2 mm fraction) was then sent to Bureau Veritas (formerly Acme) Analytical Laboratories Ltd. (Vancouver, Canada) for analysis. Samples were digested in a modified Aqua Regia solution (2 parts HCl + 2 parts HNO_3 + 2 parts distilled water) and analyzed using a combination of ICP-MS (Inductively Coupled Plasma Mass Spectrometry) and ICP-ES (Inductively Coupled Plasma Emission Spectrometry) to determine the concentration of 52 elements. These elements include Mo, Cu, Pb, Zn, Ag, Ni, Co, Mn, Fe, As, U, Au, Th, Sr, Cd, Sb, Bi, V, Ca, P, La, Cr, Mg, Ba, Ti, B, Al, Na, K, W, Sc, Tl, S, Hg, Se, Te, Ga, Cs, Ge, Hf, Nb, Rb, Sn, Zr, Y, Ce, In, Re, Be, Li, Pd, and Pt.

3.2. Anthropigene method

The geochemical gene proposed by Yan et al. (Yan et al., 2018) provides a robust framework for identifying and differentiating geochemical anomalies by comparing samples with natural background materials through specific indicator elements. Based on the above concept, the anthropigene method was developed to address anthropogenic contamination in environmental contexts, focusing on distinguishing urban and agricultural sources of pollution. The technique follows a well-established operational sequence: (1) selection of elements, (2) determination of reference values, (3) construction of spectral lines, (4) generation of "ideal gene" codes of uncontaminated soils (Anthropigenes), and (5) estimation of similarity percentages between anthropigenes and sample genes.

The first step in constructing the anthropigene involves selecting critical elements to differentiate between natural and anthropogenic inputs. Six immobile elements—Fe, U, Th, La, Ti, and Al—were chosen due to their relative stability during weathering processes, as documented in prior studies (Dosseto et al., 2019; Ma et al., 2019; Gong et al., 2011). These elements are considered reliable markers of natural geological conditions, as they are less likely to be mobilized under typical environmental conditions, although extreme weathering can lead to some degree of mobility (Frierdich and Catalano, 2012; Pokrovski et al., 2006).

Five additional indicator elements were selected to capture anthropogenic influences: Pb, Zn, Au, Sb, and Hg for urban contamination; Cu, As, P, Na, and K for agricultural contamination. These elements reflect typical urban pollution sources, such as vehicular emissions, industrial activities, waste mismanagement, and agrarian practices involving fertilizers, pesticides, and fungicides (De Vivo et al., 2021; Rashid et al., 2023; FAO and UNEP, 2021).

According to Li et al. (Li et al., 2019), average values for each element were calculated for the four major lithotypes of the Campania region reported in the framework of this paper as siliciclastic units, carbonate units, alluvial, lacustrine, and coastal units (referenced in the text as "alluvial units"), and volcanic units (Table 1). In uncontaminated environments, the values of the six immobile elements remain consistently unchanged, reflecting their stability under natural geochemical conditions. Conversely, the five indicator elements representing anthropogenic inputs, such as urban or agricultural contamination, show significant enrichment in contaminated areas while remaining low in natural conditions. This disparity forms the basis for distinguishing natural geochemical variability from anthropogenic influences.

3.2.1. Immobile elements

The reference values of the six immobile elements (Al, Fe, La, Th, Ti, and U) are determined based on the four lithotypes as follows:

1. Select the minimum value for each immobile element (Table 1) among the average values calculated for the four lithotypes and calculate the relative logarithmic values (base 10) (lgCmin);
2. Subtract 0.1 from each lgCmin; 0.1 is commonly selected according to the accuracy tolerance of analytical quality for geological samples (Yan et al., 2018).
3. Determine the reference value for each immobile element (C[*Imm*] ref) using the following equation [Eq. (1)]:

$$C[Imm]_{ref} = 10^{(\lg Cmin - 0.1)} \quad (1)$$

The calculated reference values for Campania are reported in Table 1.

3.2.2. Indicator elements

The reference values of the five indicator elements are determined as follows:

1. Select the maximum value for each indicator element (Table 1) among the average values of the four lithotypes and calculate the relative logarithmic values (base 10) (lgC_{max});
2. Add 0.1 to each lgC_{max} (Yan et al., 2018);
3. Determine the reference value for each indicator element ($C[Ind]_{ref}$) through the following equation [Eq. (2)]:

$$C[Ind]_{ref} = 10^{(\lg Cmax + 0.1)} \quad (2)$$

Concerning the Campania region, the reference values calculated for Au, Hg, Pb, Sb, and Zn (urban) and As, Cu, K, Na, and P (agricultural) are reported in Table 1.

3.2.3. Sequencing of elements

The log-ratio between the average values for each of the eleven elements and their corresponding reference values is calculated based on individual lithotypes. The values are plotted as a spider diagram, namely a spectral line (Rollinson, 1993) (Fig. 2). Specifically, to construct the spectral line for both of the anthropigenes (urban and agricultural), the following steps were performed:

Table 1
Average values for immobile and mobile elements calculated in relation to the major lithotypes of the Campania region and separated according to the urban and agricultural land use. Estimated reference values are reported in bold. Units are in mg/kg except for Au and Hg reported in μg/kg.

Urban land use	Immobile elements						Indicator elements				
Lithotypes	Al	Fe	La	Th	Ti	U	Au	Hg	Pb	Sb	Zn
siliciclastic units	24,586	23,389	25.2	7.6	363.5	1.3	3.9	41.4	30.9	0.5	75.6
volcanic units	44,750	25,513	46.4	14.3	1355.5	4.0	14.4	120.7	79.6	1.1	122.8
carbonate units	25,935	23,426	30.0	5.8	330.9	1.7	4.5	78.7	32.4	0.6	80.0
alluvial, lacustrine, coastal units	39,172	24,439	38.7	11.5	1109.1	3.3	22.9	144.2	93.6	1.5	148.1
Reference values (C_{ref})	**19,529**	**18,578**	**20.0**	**4.6**	**262.8**	**1.1**	**28.9**	**181.5**	**117.9**	**1.9**	**186.5**

Agricultural land use	Immobile elements						Indicator elements				
Lithotypes	Al	Fe	La	Th	Ti	U	As	Cu	K	Na	P
siliciclastic units	24,586	23,389	25.2	7.6	363	1.3	7.7	47.4	4893	568	823.4
volcanic units	44,750	25,513	46.4	14.3	1355	4.0	13.8	126.5	16,972	4583	1833.5
carbonate units	25,935	23,426	30.0	5.8	331	1.7	9.0	46.6	2361	153	852.6
alluvial, lacustrine, coastal units	39,172	24,439	38.7	11.5	1109	3.3	12.2	110.1	12,761	3500	1789.1
Reference values	**19,529**	**18,578**	**20**	**4.6**	**263**	**1.1**	**17.3**	**159**	**21,367**	**5769**	**2308**

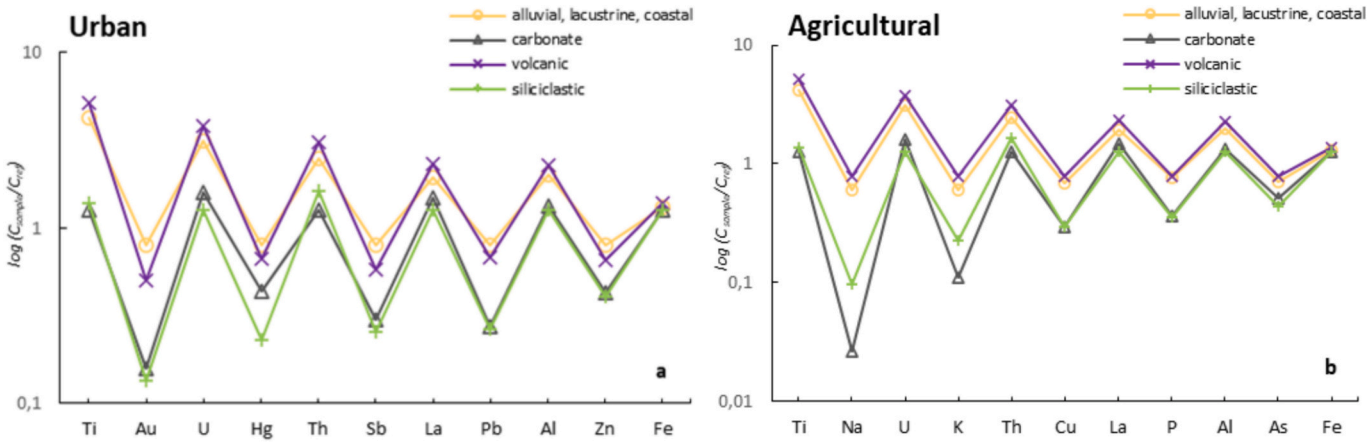

Fig. 2. Spectral lines of urban and agricultural anthropigene in different geological materials for a) urban gene and b) agricultural gene.

1) Calculate the range of the log-ratios for each element for the four geological units;
2) Arrange the six immobile elements (Ti, U, Th, La, Al, Fe) in descending order based on their ranges;
3) Similarly, arrange the five indicator elements in descending order based on their ranges, as well; for the Campania region, we have a) Au, Hg, Sb, Pb, Zn for the urban anthropigene; b) Na, K, Cu, P, As for the agricultural anthropigene;
4) Alternate one indicator element with one immobile element following the respective orders for each anthropigene; in our case:

Urban: Ti, Au, U, Hg, Th, Sb, La, Pb, Al, Zn, Fe.
Agricultural: Ti, Na, U, K, Th, Cu, La, P, Al, As, Fe.

Based on the data used in this study, the spectral lines generated for the urban and agricultural anthropigenes are presented in Fig. 2.

3.2.4. Construction of the anthropigene code

For each anthropigene, spectral lines are transformed into their corresponding gene code, according to Yan (Yan et al., 2018). The code is eleven numbers in length and begins with the number 1; the following numbers will be 0, 1, or 2 based on the difference (Δ_i) between two adjacent values [Eq. (3)]:

$$\Delta_i = \lg(C_i)_N - \lg(C_{i-1})_N \quad (3)$$

where *i* is the sequence number of the elements (from 2 to 11) and *N* is the corresponding value in the spectral line.

Based on Δ_i, a number (g_i) is assigned to the elements in the gene code, according to the following rules:

- $g_i = 2$, if $\Delta_i > 0.1$;
- $g_i = 1$ if $-0.1 \leq \Delta_i \leq 0.1$;
- $g_i = 0$ if $\Delta_i < -0.1$.

where *i* is from 2 to 11, and the value of g_i is only 0, 1, or 2 in the gene code.

For both the urban and agricultural anthropigenes, the codes equal 10,202,020,202 for all the lithotypes.

3.2.5. Sample similarity

The ultimate step is to evaluate the similarity of individual soil samples with the anthropigenes.

First, the urban and agricultural sample gene codes have to be determined for each topsoil. They are calculated using the same approach applied for the anthropigene using the specific concentration values of the selected elements and the reference values in Table 1.

Subsequently, Eqs. (3) and (4) are applied to build the code. The sample gene code is compared with the urban and agricultural anthropigene codes, considering the geological unit where the samples fall. By chance, in the present study, the anthropigene codes are the same for all the geological units.

For each element, the degree of similarity (Rd_i) of individual samples with the anthropigene is determined as follows:

- $Rd_i = 1$, if the values of g_i are the same;
- $Rd_i = 0.5$, if the values of g_i are adjacent (1 and 0, or 1 and 2);
- $Rd_i = 0$, if the values of g_i are not adjacent (2 and 0, or 0 and 2).

Finally, the similarity (R) between a sample gene and the anthropigene codes is calculated as [Eq. (4)]:

$$R = \frac{\sum_{i=2}^{n} R_{gi}}{n-1} \times 100\% \quad (4)$$

where n is 11, and the value of R ranges between 0 % and 100 %.

If the similarity is 80 %, the sample features one indicator element enriched compared to the anthropigene. Similarly, in the case of two indicator elements enriched in a sample, the similarity will decrease to 60 %, and so on. Therefore, we can use the similarity between a sample and the anthropigene to estimate its degree of contamination.

The sample gene codes for the 3182 topsoils of the Campania region were calculated through a script developed by authors using the programming environment of R software (Supplementary Material: SM1). The similarity values were mapped through QGIS 3.22, using equal intervals (i.e., 0 %–20 %, 20 %–40 %,40 %–60 %, 60 %–80 %, 80 %–100 %) (Fig. 3).

3.3. Geochemical background assessment

Geochemical background values for the indicator elements were determined using the original dataset, deprived of those samples featuring a similarity value <80 %, deemed anomalous. Subsequently, the samples were divided based on the lithotype they belonged to, and data were transformed using the Box-Cox technique (Box and Cox, 1964) to normalize their distribution as much as possible and improve their statistical handling. The normalization operation was carried out using the "boxcox" function implemented in the "MASS" package (Venables and Ripley, 2002) available in the R software computing environment.

For each element and each referenced lithotype of the Campania region, the Upper Background Limit (UBL) was determined by first calculating the upper tolerance limit with 95 % confidence and 90 % coverage (95UTL90) on the Box-Cox transformed data using the ProUCL software (USEPA, 2022).

The UBL values (mg/kg) were then obtained by applying the inverse Box-Cox transformation to the 95UTL90s.

4. Results

For a better interpretation of the results obtained by applying the proposed method, two dot maps (one for the urban and one for the agricultural anthropigene) showing the spatial distribution of the similarity were generated (Fig. 3). Samples were classified using five equal intervals covering each a range of 20 %. The 0–20 % similarity interval indicates the highest degree of contamination, meaning all five indicator elements significantly deviate from their reference. Conversely, the 80–100 % interval features samples with low or almost absent contamination, as anthropic sources influence none or, at most, one indicator element.

Out of the 3182 topsoil samples analyzed concerning the urban anthropigene, the distribution of samples across the similarity intervals is as follows (Fig. 3a):

- 0–20 % similarity interval: 28 samples;
- 20–40 % similarity interval: 38 samples;
- 40–60 % similarity interval: 94 samples;
- 60–80 % similarity interval: 192 samples;
- 80–100 % similarity interval: 2830 samples.

The samples characterized by the lowest similarity values (0–20 %), indicating significant environmental alteration due to anthropogenic factors, are primarily located in correspondence with the downtown of the region's major urban and industrial centers, namely Naples and Salerno (Fig. 3b, c). Moderate contamination (20–40 % similarity) features the suburbs of the cities as well as the main regional transport routes. The similarity classes of 40–60 % and 60–80 %, corresponding to progressively lower contamination degrees, characterize samples proceeding from areas predominantly located on the external edges of major urban centers and consisting of rural or semi-rural landscapes. Finally, samples with the highest similarity (80–100 %), indicating minimal contamination, are widespread in correspondence with inner and/or mountainous regions far from urbanization.

Concerning the agricultural anthropigene, a total of 3405 samples were analyzed, and they are spanned across the similarity intervals as follows (Fig. 3d):

- 0–20 % similarity interval: 0 samples;
- 20–40 % similarity interval: 1 sample;
- 40–60 % similarity interval: 37 samples;
- 60–80 % similarity interval: 349 samples;
- 80–100 % similarity interval: 3018 samples.

The slight difference in the number of samples analyzed for the two anthropigenes is due to the absence of concentration data for some of the selected elements in a portion of the initial dataset.

In this case, the data highlights the prevalence of high similarity values (80–100 %), which is even higher than that related to urban pressure, indicating limited contamination across the region. Areas with extremely high agricultural contamination (0–20 % similarity interval) are absent, with relevant contamination (20–40 % similarity interval) primarily near Benevento. Moderate contamination levels (40–60 % and 60–80 % similarity intervals) are observed in rural and peri-urban areas, particularly around Caserta, Avellino, and Salerno, and correspondence with Ischia Island, Vesuvius slopes, and the Sarno River plain (Fig. 3e, f). In contrast, areas with 80–100 % similarity are predominantly located in mountainous and rural regions, indicating minimal or no contamination, associated with low levels of human activity or traditional farming practices.

As reported above, for assessing the UBLs of the indicator elements for the main regional lithotypes (Table 2), samples within the 80–100 % similarity interval for both the urban and agricultural anthropigene were selected (Fig. 4).

Considering the indicator elements used for the urban anthropigene:

- The highest UBL values of Pb were determined for the alluvial (150 mg/kg) and the volcanic (142 mg/kg) units, while the lowest value features the siliciclastic units with 69.08 mg/kg.
- Zn UBLs show a clear separation between soils developed on volcanic and alluvial units (at 238 and 234 mg/kg, respectively) and those related to sedimentary lithotypes, with siliciclastic and carbonatic units characterized by 131 and 133 mg/kg, respectively.
- Au is characterized by the highest UBL for the soil of the alluvial units (36 μg/kg), followed by the volcanic unit at 33.1 μg/kg and, at a distance, by sedimentary lithotypes.
- Sb remains relatively low, with its highest UBL values featuring the alluvial units and carbonate lithotypes at 2.27 and 4.25 mg/kg, respectively.
- Hg has its highest UBL in the soil of the alluvial units (353 μg/kg) and its lowest value on siliciclastic materials, like Zn and Au.

For the agricultural gene indicator elements:

- Cu UBLs peak in soils developed on alluvial, lacustrine, and coastal units (275 mg/kg) and volcanic materials (257 mg/kg) with markedly lower values for sedimentary units.

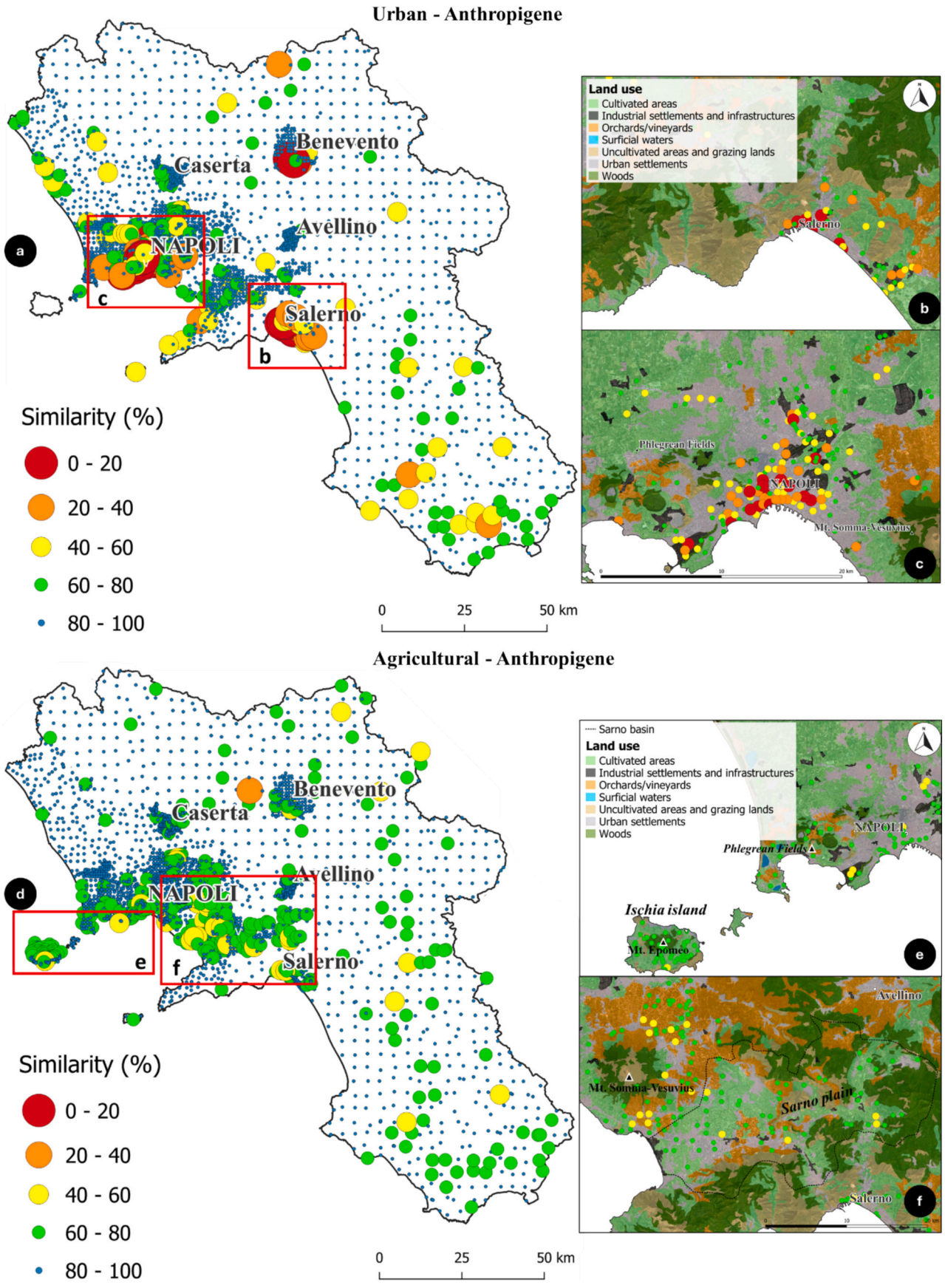

Fig. 3. Spatial distribution of similarity classes for urban (a, b, c) and agricultural anthropigenes (d, e, f) in the Campania region. The red boxes highlight areas that are subsequently zoomed in on the right-hand side of the figure. (For interpretation of the references to colour in this figure legend, the reader is referred to the web version of this article.)

Table 2
UBLs estimated for the indicator elements concerning major lithotypes of Campania.

Lithotype	Pb (mg/kg)	Zn (mg/kg)	Au (μg/kg)	Sb (mg/kg)	Hg (μg/kg)	Cu (mg/kg)	As (mg/kg)	P (mg/kg)	Na (mg/kg)	K (mg/kg)
Siliciclastic units	69.08	131	9.2	1.09	89.8	112.11	17.99	1702	2110	1478
Volcanic units	142	238	33.1	2.02	337	257	23	3658	10,967	37,790
Alluvial units	150	234	36	2.27	353	275	22	3871	10,219	34,858
Carbonatic units	81	133	15	4.25	243	113	47	2241	2762	5330

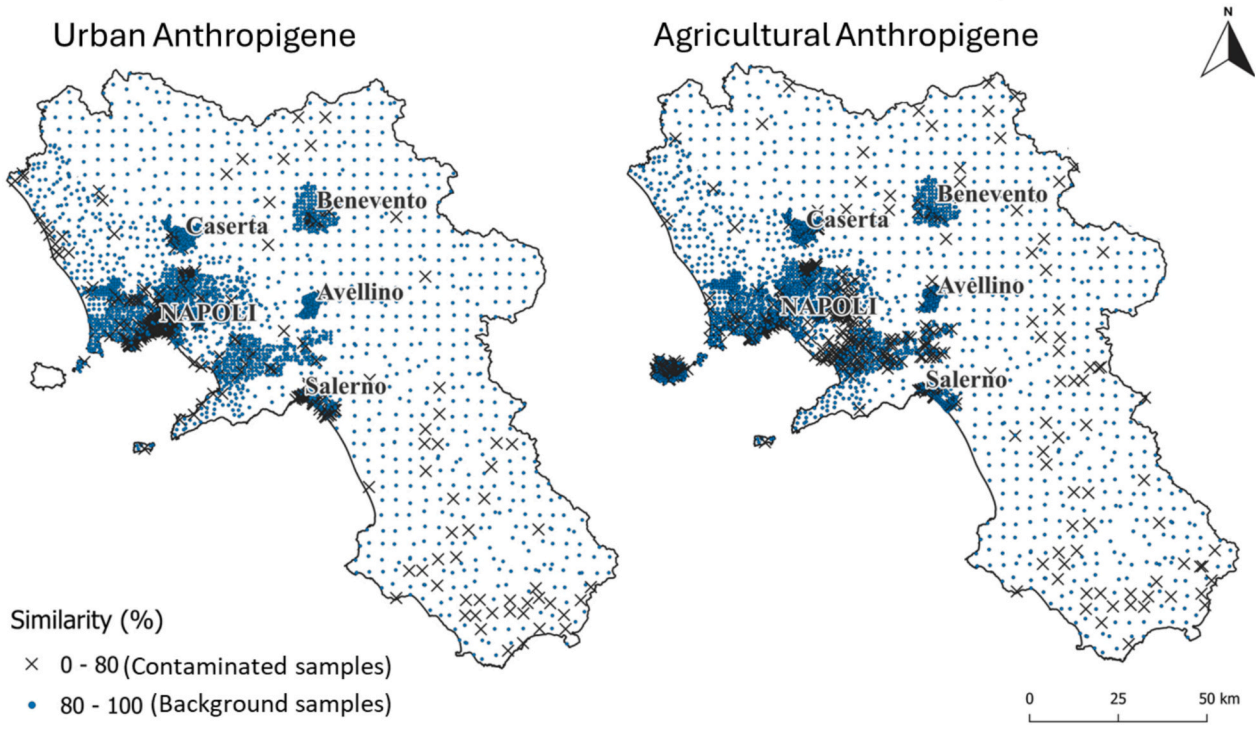

Fig. 4. Spatial distribution of Background topsoil samples.

- As shows an almost homogeneous distribution across the four lithological units, with slightly higher values for carbonate units (47 mg/kg).
- P presents more marked UBL values in the alluvial and volcanic units (3871 and 3658 mg/kg, respectively) and the lowest values in correspondence with the siliciclastic units (1702 mg/kg).
- Na shows exceptionally high UBLs in the volcanic and alluvial units (10,967 and 10,219 mg/kg, respectively) in contrast to the sedimentary units, which instead present relatively low values (2762 mg/kg for carbonate units and 2110 mg/kg for siliciclastic units).
- K, similarly to Na, reaches its highest UBL values in the volcanic and alluvial units (37,790 and 34,858 mg/kg, respectively), in contrast to siliciclastic units featuring extremely low values (1478 mg/kg) in relation to the other units.

5. Discussions

The analysis of the similarity distribution with the urban anthropigene for Campania soils reveals a pronounced contamination gradient associated with urban and industrial areas. It is important to note that the similarity index is based on the background gene reference. Therefore, areas with lower similarity values represent zones with higher degrees of anthropogenic impact. Conversely, more remote and mountainous regions exhibit minimal or no contamination, likely due to their reduced exposure to anthropogenic pressures. In urban areas, similarity values (0–20 %) can be attributed to anthropogenic sources linked to the selected indicator elements (Pb, Zn, Au, Sb, and Hg) commonly associated with industrial processes and urban pollution sources. Pb is frequently related to vehicular emissions, paints used in older buildings, and improper industrial waste management. Similarly, Zn is released into the atmosphere and deposited on the soil by metallurgical activities, galvanic processes, fossil fuel combustion, and tire consumption, making it a major environmental contaminant in densely populated urban areas (Zuzolo et al., 2017; de Almeida Ribeiro Carvalho et al., 2022; Cicchella et al., 2020; Nawrot et al., 2020).

Au and Sb can be traced back to specific industrial activities such as precious metal processing, alloy production, and electronics manufacturing, but they can also be associated with catalytic converters in motor vehicles. Although these elements are relatively rare in nature, they tend to accumulate in the soil of industrialized and/or highly populated areas due to emissions from production sites and improper disposal of waste containing these substances (Wang and Qin, 2006; Dupont et al., 2016; Ding et al., 2019; Yan et al., 2020). Lastly, Hg contamination is often due to the historical use of this element in industrial and mining processes and coal combustion (Feng et al., 2002; Selin, 2009). Urban sources of Hg also include emissions from chlor-alkali and electronic industries and crematoria (Davies et al., 1986; Southworth et al., 2004; Lim and Schoenung, 2010).

The distribution of these elements in the topsoil of Campania's urban areas thus reflects the environmental pressure exerted by anthropogenic activities and industrial processes, creating a clear distinction between the most impacted urban zones and less affected areas of the region.

The background values, determined for soils developed on the four considered lithotypes (Table 2), represent the chemical elements'

natural concentrations, primarily reflecting the lithological and mineralogical characteristics of each unit and the natural weathering processes occurring to them.

Indeed, Pb UBLs feature their highest level in the alluvial unit due to the accumulation of sediment proceeding from volcanic areas and layers of organic matter typical of alluvial environments (Dewey et al., 2021; Izquierdo et al., 2012). Zn UBLs distribution confirms a natural presence of the element in the volcanic soils of Campania (Zuzolo et al., 2020) and in soils developed on transported sediments (alluvial units) fed by the products of the weathering of volcanic units. Similarly to Pb and Zn, Au UBLs, which are higher in soils of the volcanic and alluvial units, depend on the different compositional nature of the source rocks (Pitcairn, 2011). Sb UBLs show reduced variability in Campanian soils, probably due to the generally low content of this element in the regional lithotypes. The slightly higher UBL value for soils associated with carbonate units can be related to their relative stability and the presence of an acidic environment (Diquattro et al., 2021), promoted by the presence of organic matter in soils of the Apennine reliefs commonly associated with the widespread coverage of woods (Fig. 1b).

Finally, Hg UBLs show increased values in the alluvial and volcanic units, probably due to the natural enrichment of this element in volcanic materials (Peña-Rodríguez et al., 2012) and the higher organic content and specific adsorption properties of sediment in the floodplain zones (Gervais-Beaulac et al., 2013).

The spatial analysis of the similarity with the agricultural anthropigene (Fig. 3d) highlights a clear difference between areas featuring a high pressure from agriculture, associated with contamination due to indicator elements (Na, K, P, Cu, and As), and others unaffected by human action.

The slopes of Mt. Somma-Vesuvius, the Phlegraean field area, the island of Ischia, and the Sarno River plain (Fig. 3e, f) are affected by a more spatially homogeneous contamination from agricultural practices. However, the similarity values do not fall below 40 %, suggesting a moderate impact of agriculture on soil chemical alteration.

The southeastern slopes of Vesuvius represent an area where agriculture thrives due to the fertility of volcanic soils. Here, typical products and various high-quality horticultural and fruit crops are cultivated (e.g., Piennolo tomatoes and apricots), reflecting the local biodiversity (Tranchida-Lombardo et al., 2018; Carillo et al., 2019; Fratianni et al., 2022). The mineral-rich composition of volcanic soil ensures high-quality yields. It supports the sustainable agricultural tradition of the Mt. Somma-Vesuvius area, including viticulture (Ciriminna et al., 2022), although the use of biological Cu-based fungicides (Komárek et al., 2010; Roviello et al., 2021) and fertilizers containing (among other elements) K and P (Randall and Hoeft, 1988) cannot be avoided.

Similarly, the contamination determined for the Phlegraean Fields and Ischia Island can be explained by a renowned wine-making tradition, supported by volcanic soils with peculiar mineralogical characteristics and an ideal microclimate for vine cultivation (Pollini et al., 2013).

The Sarno river plain, one of the most fertile areas in the Campania region, featuring a low to moderate level of contamination, is the growing zone of the San Marzano tomato, regarded as an Italian excellence (Rao et al., 2006; Raimondi et al., 2021). The contamination highlighted by the similarity analysis is potentially attributable to environmental pressures arising from intensive agriculture. The river plain is characterized by greenhouses and high-yield farming, supported by abundant water resources and extremely productive alluvial soils (Montuori et al., 2013; Cicchella et al., 2014).

Similar to Pb (included in the urban anthropigene sequence), the distribution of Cu UBLs, showing a clear separation between values associated with alluvial and volcanic units and the siliciclastic and carbonatic lithotypes, suggests a strong influence exerted on the overall variability by the spreading of regional volcanism products (Fig. 1a). On the contrary, As, featuring widespread homogeneous UBLs across the regional territory (probably due to its limited content in local lithotypes), only shows a spike in correspondence with the carbonate units; this behavior is possibly due to the weathering (associated with the Mediterranean climate) of the bedrock containing iron minerals usually carrying As (Xia et al., 2024).

The general common trend of soil UBLs' variability shown by macronutrients included in the agricultural anthropigene (i.e., P, Na, and K) is mainly related, as for some of the considered trace elements, to the underlying presence (or absence) of volcanic materials and their transported alteration products (alluvial units).

Understandably, the difference in K UBLs between volcanic and alluvial units and sedimentary units (siliciclastic and carbonate) is particularly marked due to the alkaline nature of the regional magmatic activity (De Vivo et al., 2020).

The results of the procedure used to determine UBLs through the method developed in this study were compared with those based on the application of the “Guideline for the determination of background values for soils and groundwaters” issued by the Italian National Environmental Protection System (SNPA, 2018) (from now referenced in the text as “SNPA method”). In the SNPA method, the process begins with the removal of outliers (or anomalous values) through a univariate statistical analysis of the data distribution based on boxplot (Supplementary Material: SM2, SM3) and QQ-plot diagrams (Supplementary Material: SM4) (Albanese et al., 2007; Reimann and Filzmoser, 2000). The Q-Q plots were created for this paper in the R software environment using the “qqPlot” function available in the “car” package (Fox and Weisberg, 2019), utilizing the data normalized via the Box-Cox transformation.

Subsequently, for the assessment of the UBLs, the “refined” dataset undergoes the same treatment applied to the data extracted using the “similarity criteria” (i.e., values >80 %) proposed in this work.

The comparison, hence, aimed to determine whether there were significant differences in the distribution and mean values of the datasets generated through the application of the two different approaches (i.e., the “similarity criteria” and “SNPA” methods).

To this end, Welch's *t*-test for independent samples, a robust statistical test that assumes unequal variances between two groups (Table 3) (West, 2021), was applied. The test is based on comparing the means of the two datasets and identifying any statistically significant discrepancies between them.

The analysis was conducted using JASP software (version 0.18.3.0). The test result is commonly reported in terms of “*p*-value.” If the resulting p-value exceeds the significance level ($\alpha = 0.05$), it indicates no statistically relevant difference between the two groups compared. Conversely, if the p-value <0.05, a significant difference is expected among the groups.

In our case, detecting a significant difference among the datasets generated by applying the similarity criteria and SNPA methods led to the assumption that the UBLs generated based on them were also significantly different.

In the specific case of the urban indicator elements, the results revealed statistically significant differences among the distribution of Pb, Zn, Au, Sb, and Hg generated by the two methods (p-value<0.05) (Table 3). Specifically, focusing on the geochemical background of these elements and individual lithotypes:

- For the siliciclastic units, UBLs of Pb (69.08 mg/kg versus 69.07 mg/kg) and Zn (131 mg/kg versus 126 mg/kg) resulted almost the same despite the Welch's t-test suggesting a significant difference among the distribution of the datasets generated by applying the similarity criteria and the SNPA method. Similarly, Hg exhibits a slight discrepancy between values (89.8 μg/kg versus 94.8 μg/kg), though the UBLs remain comparable.
- A pronounced deviation was observed for the UBLs of Pb (142 mg/kg versus 201 mg/kg), Zn (238 mg/kg versus 285 mg/kg), Au (33.1 μg/kg versus 44.8 μg/kg), and Hg (337 μg/kg versus 438 μg/kg) for the

Table 3
UBL values estimated for urban and agricultural indicator elements, using the refined datasets obtained by applying the Similarity criteria (this paper)and the SNPA method (SNPA, 2018). The Welch's *t*-test for independent samples was performed to assess significant statistical differences between the results based on the two approaches (p-value <0.05). Elements featuring significant differences in distributions are reported in bold.

Lithotypes	UBLs (Urban indicator elements)		Welch's t-test
	Similarity criteria (this paper)	SNPA method (SNPA, 2018)	p-value (α = 0.05)
Siliciclastic units			
Pb (mg/kg)	69.08	69.07	< 0.05
Zn (mg/kg)	131	126	< 0.05
Au (μg/kg)	9.2	7.5	0.901
Sb (mg/kg)	1.09	1.17	0.465
Hg (μg/kg)	89.8	94.8	< 0.05
Volcanic units			
Pb (mg/kg)	142	201	< 0.05
Zn (mg/kg)	238	285	< 0.05
Au (μg/kg)	33.1	44.8	< 0.05
Sb (mg/kg)	2.0	2.8	0.94
Hg (μg/kg)	337	438	< 0.05
Alluvial units			
Pb (mg/kg)	150	236	< 0.05
Zn (mg/kg)	234	392	< 0.05
Au (μg/kg)	36	75	0,98
Sb (mg/kg)	2.27	5.6	< 0.05
Hg (μg/kg)	353	563	< 0.05
Carbonate units			
Pb (mg/kg)	81	77	0,055
Zn (mg/kg)	133	150	< 0.05
Au (μg/kg)	15	18	0,815
Sb (mg/kg)	4.2	1.8	0,485
Hg (μg/kg)	243	272	< 0.05

Lithotypes	UBLs (Agricultural indicator elements)		Welch's t-test
	Similarity criteria (this paper)	SNPA method (SNPA, 2018)	p-value (α = 0.05)
Siliciclastic units			
Cu (mg/kg)	112.11	95.44	< 0.05
As (mg/kg)	17.99	16.13	< 0.05
P (mg/kg)	1700	1600	< 0.05
Na (mg/kg)	2100	1800	< 0.05
K (mg/kg)	14,000	10,200	< 0.05
Volcanic units			
Cu (mg/kg)	257	414	< 0.05
As (mg/kg)	23	22	< 0.05
P (mg/kg)	3600	4200	< 0.05
Na (mg/kg)	10,900	11,400	< 0.05
K (mg/kg)	37,700	45,200	< 0.05
Alluvial units			
Cu (mg/kg)	275	329	< 0.05
As (mg/kg)	22	21	0.085
P (mg/kg)	3800	3900	< 0.05
Na	10,200	10,200	< 0.05
K	34,600	35,300	< 0.05
Carbonate units			
Cu (mg/kg)	113	139	< 0.05
As (mg/kg)	47	33	0.924
P (mg/kg)	2200	2600	< 0.05
Na (mg/kg)	2700	1400	< 0.05
K (mg/kg)	5300	4700	< 0.05

volcanic units, with increasingly higher values for the datasets generated by applying the SNPA method.

- For the alluvial units, UBLs of Pb (150 mg/kg versus 236 mg/kg), Zn (234 mg/kg versus 392 mg/kg), Sb (2.27 mg/kg versus 5.60 mg/kg), and Hg (353 μg/kg versus 563 μg/kg) display notable differences among the values, with values based on the SNPA method generally higher.
- The UBL values of Zn (133 mg/kg versus 150 mg/kg) and Hg (243 μg/kg versus 272 μg/kg) exhibited moderate deviations for the carbonate units.

Significant changes were found for all the agricultural indicator elements, except for As in the case of alluvial (p-value = 0.085) and carbonate (p-value = 0.924) units.

Concerning geochemical backgrounds for the considered lithotypes:

- In the siliciclastic units, Cu and As UBLs exhibit slightly higher values for the dataset generated by applying the similarity criteria (112.11 mg/kg for Cu, 17.99 mg/kg for As) than for the one based on the SNPA method (95.44 mg/kg for Cu, 16.13 mg/kg for As). For major elements (P, Na, and K), the UBLs from the dataset produced using samples with a similarity >80 % are generally higher, though no wide variations are observed.
- For the volcanic units, a more marked difference is observed among the UBLs of Cu, with a much higher value for the dataset produced through the SNPA method (414 mg/kg) than the one based on the similarity criteria (257 mg/kg). While As UBLs feature no substantial changes (23 mg/kg versus 22 mg/kg, respectively), major elements (P, Na, and K) consistently yield higher UBLs in the SNPA-based data, showing variable differences. Particularly, Na (10,900 mg/kg versus 11,400 mg/kg) and K (37,700 mg/kg versus 45,200 mg/kg) present notable discrepancies.
- For the alluvial units, the trend for Cu remains similar, with the SNPA method producing higher UBLs (329 mg/kg) compared to the similarity criteria (275 mg/kg). Significant changes are seen for P and K, while Na presents the same UBL values (10,200 mg/kg) across both datasets.
- Cu UBL is higher in the SNPA dataset (139 mg/kg) for the carbonate units than in the similarity-based dataset (113 mg/kg). Arsenic, Na, and K UBLs are higher for the similarity criteria dataset (47 mg/kg for As, 2700 mg/kg for Na, and 5300 mg/kg for K) compared to the SNPA method (33 mg/kg for As, 1400 mg/kg for Na, 4700 mg/kg for K). P (2,200 mg/kg versus 2600 mg/kg) shows higher UBL values in the SNPA dataset.

In summary, the UBL values calculated using datasets produced through the similarity criteria tend to be generally lower and more conservative than those generated by the Italian guidelines. Their enhanced conservativeness is crucial for applications aimed at tier-one human health risk assessments or as a target for environmental remediation and restoration of contaminated sites. Importantly, these conservative values are not simply based on precautionary limits but are derived through a more comprehensive and multivariate analysis of contamination sources, based on representative contaminant groups rather than isolated elements.

6. Conclusions

This work presents a methodological advancement in the spatial analysis of contamination processes, introducing an approach based on the quantification of deviations from geochemical background conditions through the concept of anthropigene similarity.

The integration of multiple contamination indicators enables a more robust classification of soils compared to traditional methods, enhancing the reliability of baseline definition and anomaly identification.

The main results obtained are summarized as follows:

1. The proposed method enables a more accurate spatial interpretation of contamination processes, effectively distinguishing between urban and agricultural sources;
2. Compared to conventional approaches, the analysis based on anthropigene similarity demonstrates higher sensitivity and greater discriminative power;

3. The application of the proposed procedure for the determination of the UBLs proved valuable not only for local applications (risk assessment, remediation, and management of contaminated sites) but also for the identification of large-scale diffuse contamination phenomena that might otherwise be attributed to natural enrichments, as observed in the case studies of Ischia Island and the Sarno River basin.

The method has wide margins for improvement. Future studies will focus on identifying specific indicators of anthropic processes not considered in this paper and improving techniques for estimating background values.

Supplementary data to this article can be found online at https://doi.org/10.1016/j.gexplo.2025.107832.

CRediT authorship contribution statement

Lucia Rita Pacifico: Writing – original draft, Software, Methodology, Investigation, Formal analysis, Data curation, Conceptualization. **Francesco Carotenuto:** Software, Data curation. **Annalise Guarino:** Validation. **Antonio Iannone:** Investigation, Data curation. **Domenico Cicchella:** Validation. **Stefano Albanese:** Writing – original draft, Supervision, Resources, Funding acquisition, Conceptualization.

Declaration of competing interest

The authors declare that they have no known competing financial interests or personal relationships that could have appeared to influence the work reported in this paper

Acknowledgments

This study was carried out within the RETURN Extended Partnership and received funding from the European Union NextGenerationEU (National Recovery and Resilience Plan (NRRP), Mission 4, Component 2, Investment 1.3—D.D. 1243 2/8/2022, PE0000005).

Data availability

Data will be made available on request.

References

Adriano, D.C., 2001. Trace elements in terrestrial environments: biogeochemistry, bioavailability, and risks of metals. Springer.

Albanese, S., De Vivo, B., Lima, A., Cicchella, D., 2007. Geochemical background and baseline values of toxic elements in stream sediments of Campania region (Italy). J. Geochem. Explor. 93, 21–34. https://doi.org/10.1016/j.gexplo.2006.07.006.

Alloway, B.J., 2012. Heavy metals in soils: trace metals and metalloids in soils and their bioavailability. Springer.

de Almeida Ribeiro Carvalho, M., Botero, W.G., de Oliveira, L.C., 2022. Natural and anthropogenic sources of potentially toxic elements to aquatic environment: a systematic literature review. Environ. Sci. Pollut. Res. 29, 51318–51338. https://doi.org/10.1007/s11356-022-20980-x.

ARPAC, Agenzia Regionale per la Protezione dell'Ambiente Campania, 2021. Environmental Report of Campania. https://www.regione.campania.it/assets/documents/rapporto-ambientale-deliberazioni-della-giunta-regionale-agc-05.pdf (in Italian).

Box, G.E.P., Cox, D.R., 1964. An analysis of transformations. J. R. Stat. Soc. B. Methodol. 26 (2), 211–252.

Buccianti, A., Lima, A., Albanese, S., Cannatelli, C., Esposito, R., De Vivo, B., 2015. Exploring topsoil geochemistry from the CoDA (Compositional Data Analysis) perspective: the multi-element data archive of the Campania Region (Southern Italy). J. Geochem. Explor. 159, 302–316.

Carillo, P., Kyriacou, M.C., El-Nakhel, C., Pannico, A., dell'Aversana, E., D'Amelia, L., Colla, G., Caruso, G., De Pascale, S., Rouphael, Y., 2019. Sensory and functional quality characterization of protected designation of origin 'Piennolo del Vesuvio' cherry tomato landraces from Campania-Italy. Food Chem. 292, 166–175. https://doi.org/10.1016/j.foodchem.2019.04.056.

Cheng, Q., Agterberg, F.P., Ballantyne, S.B., 1994. The separation of geochemical anomalies from background by fractal methods. J. Geochem. Explor. 51, 109–130. https://doi.org/10.1016/0375-6742(94)90013-2.

Cicchella, D., Giaccio, L., Lima, A., Albanese, S., Cosenza, A., Civitillo, D., De Vivo, B., 2014. Assessment of the topsoil heavy metals pollution in the Sarno River basin, South Italy. Environ. Earth Sci. 71, 5129–5143.

Cicchella, D., Zuzolo, D., Albanese, S., Fedele, L., Di Tota, I., Guagliardi, I., Thiombane, M., De Vivo, B., Lima, A., 2020. Urban soil contamination in Salerno (Italy): Concentrations and patterns of major, minor, trace, and ultra-trace elements in soils. J. Geochem. Explor. 213. https://doi.org/10.1016/j.gexplo.2020.106519.

Ciriminna, R., Scurria, A., Tizza, G., Pagliaro, M., 2022. Volcanic ash as multi-nutrient mineral fertilizer: science and early applications. ChemRxiv. https://doi.org/10.26434/chemrxiv-2022-brsxc.

Davies, S.P., Kassab, J.Y., Thrush, A.J., Smith, P.H., 1986. A comparison of mercury and digital clinical thermometers. J. Adv. Nurs. 11 (5), 535–543. https://doi.org/10.1111/j.1365-2648.1986.tb01285.x.

De Vivo, B., Lima, A., Albanese, S., Cicchella, D., Rezza, C., Civitillo, D., Minolfi, G., Zuzolo, D., 2016. Atlante geochimico-ambientale dei suoli della Campania. Aracne Editrice (In Italian).

De Vivo, B., Belkin, H.E., Rolandi, G., 2020. Vesuvius, Campi Flegrei, and Campanian volcanism. Elsevier. https://doi.org/10.1016/B978-0-12-816454-9.00003-1.

De Vivo, B., Cicchella, D., Lima, A., Fortelli, A., Guarino, A., Zuzolo, D., Esposito, M., Cerino, P., Pizzolante, A., Albanese, S., 2021. Monitoraggio geochimico-ambientale dei suoli della regione Campania. Progetto Campania trasparente. Volume I. Conoscenza Geochimica del Territorio. ARACNE.

Dewey, C., Bargar, J.R., Fendorf, S., 2021. Porewater lead concentrations limited by particulate organic matter coupled with ephemeral iron (III) and sulfide phases during redox cycles within contaminated floodplain sediments. Environ. Sci. Technol. 55 (9), 5878–5886. https://doi.org/10.1021/acs.est.0c08162.

Ding, Y., Zhang, S., Liu, B., Zheng, H., Chang, C.C., Ekberg, C., 2019. Recovery of precious metals from electronic waste and spent catalysts: a review. Resources, Conservation & Recycling 141, 284–298.

Diquattro, S., Castaldi, P., Ritch, S., Juhasz, A.L., Brunetti, G., Scheckel, K.G., Garau, G., Lombi, E., 2021. Insights into the fate of antimony (Sb) in contaminated soils: Ageing influence on Sb mobility, bioavailability, bioaccessibility, and speciation. Sci. Total Environ. 770, 145354. https://doi.org/10.1016/j.scitotenv.2021.145354.

Dosseto, A., Menozzi, D., Kinsley, L.P.J., 2019. Age and rate of weathering determined using uranium-series isotopes: Testing various approaches. Geochim. Cosmochim. Acta 246, 213–233.

Dupont, D., Arnout, S., Jones, P.T., 2016. Antimony recovery from end-of-life products and industrial process residues: a critical review. J. Sustain. Metall. 2, 79–103. https://doi.org/10.1007/s40831-016-0043-y.

FAO, UNEP, 2021. Global assessment of soil pollution: summary for policymakers. FAO. https://doi.org/10.4060/cb4827en.

Feng, X., Sommar, J., Lindqvist, O., Hong, Y., 2002. Occurrence, emissions, and deposition of mercury during coal combustion in the province Guizhou, China. Water Air Soil Pollut. 139, 311–324.

Fox, J., Weisberg, S., 2019. An R Companion to Applied Regression, 3rd ed. SAGE Publications https://socialsciences.mcmaster.ca/jfox/Books/Companion/.

Fratianni, F., Cozzolino, R., d'Acierno, A., Ombra, M.N., Spigno, P., Riccardi, R., Malorni, L., Stocchero, M., Nazzaro, F., 2022. Biochemical characterization of some varieties of apricot present in the Vesuvius area, southern Italy. Front. Nutr. 9, 854868. https://doi.org/10.3389/fnut.2022.854868.

Frierdich, A.J., Catalano, J.G., 2012. Distribution and speciation of trace elements in iron and manganese oxide cave deposits. Geochim. Cosmochim. Acta 91, 240–253.

Gervais-Beaulac, V., Saint-Laurent, D., Berthelot, J.S., Mesfioui, M., 2013. Organic carbon distribution in alluvial soils according to different flood risk zones. J. Soil Sci. Environ. Manag. 4 (8), 169–177.

Gong, Q., Deng, J., Yang, L., Zhang, J., Wang, Q., Zhang, G., 2011. Behavior of major and trace elements during weathering of sericite-quartz schist. J. Asian Earth Sci. 42, 1–13.

Gong, Q., Wu, X., Yan, T., Liu, N., Li, X., Li, R., Liu, M., 2020. Construction and test of geochemical genes: Case studies in China. Geoscience 34, 865–882 (In Chinese with English abstract).

Guarino, A., Lima, A., Cicchella, D., Albanese, S., 2022. Radon flux estimates, from both gamma radiation and geochemical data, to determine sources, migration pathways, and related health risk: the Campania region (Italy) case study. Chemosphere 287, 132233. https://doi.org/10.1016/j.chemosphere.2021.132233.

Izquierdo, M., Tye, A.M., Chenery, S.R., 2012. Sources, lability, and solubility of Pb in alluvial soils of the River Trent catchment, U.K. Sci. Total Environ. 433, 110–122.

Komárek, M., Čadková, E., Chrastný, V., Bordas, F., Bollinger, J.-C., 2010. Contamination of vineyard soils with fungicides: a review of environmental and toxicological aspects. Environ. Int. 36, 138–151. https://doi.org/10.1016/j.envint.2009.10.005.

Li, R., Liu, N., Gong, Q., Wu, X., Yan, T., Li, X., Liu, M., 2019. Construction, test, and application of a geochemical gold metallogene: Case studies in China. J. Geochem. Explor. 204, 1–11.

Lim, S.R., Schoenung, J.M., 2010. Human health and ecological toxicity potentials due to heavy metal content in waste electronics with flat panel displays. J. Hazard. Mater. 177, 251–259.

Ma, L., Dosseto, A., Gaillardet, J., Sak, P.B., Brantley, S., 2019. Quantifying weathering rind formation rates using in situ measurements of U-series isotopes with laser ablation and inductively coupled plasma-mass spectrometry. Geochim. Cosmochim. Acta 247, 1–26.

Matschullat, J., Ottenstein, R., Reimann, C., 2000. Geochemical background – can we calculate it? Environ. Geol. 39, 990–1000. https://doi.org/10.1007/s002549900084.

Minolfi, G., Albanese, S., Lima, A., Tarvainen, T., Fortelli, A., De Vivo, B., 2018. A regional approach to environmental risk assessment—Human health risk

assessment case study in the Campania region. J. Geochem. Explor. 184 (B), 400–416.
Montuori, P., Lama, P., Aurino, S., Naviglio, D., Triassi, M., 2013. Metal loads into the Mediterranean Sea: Estimate of Sarno River inputs and ecological risk. Ecotoxicology 22, 295–307.
Nawrot, N., Wojciechowska, E., Rezania, S., Walkusz-Miotk, J., Pazdro, K., 2020. The effects of urban vehicle traffic on heavy metal contamination in road sweeping waste and bottom sediments of retention tanks. Sci. Total Environ. 749, 141511.
Négrel, P., Ladenberger, A., Reimann, C., Birke, M., Demetriades, A., Sadeghi, M., 2019. GEMAS: geochemical background and mineral potential of emerging tech-critical elements in Europe revealed from low-sampling density geochemical mapping. Appl. Geochem. 111, 104425.
Pawlowsky-Glahn, V., Egozcue, J.J., 2006. Compositional data and their analysis: an introduction. Geol. Soc. Lond. Spec. Publ. 264 (1), 1–10.
Peccerillo, A., 2005. Plio-Quaternary volcanism in Italy, 365. Springer-Verlag Berlin Heidelberg.
Peccerillo, A., 2017. Cenozoic Volcanism in the Tyrrhenian Sea Region. Springer.
Peña-Rodríguez, S., Pontevedra-Pombal, X., Fernández-Calviño, D., Taboada, T., Arias-Estévez, M., Martínez-Cortizas, A., Nóvoa-Muñoz, J.C., García-Rodeja, E., 2012. Mercury content in volcanic soils across Europe and its relationship with soil properties. J. Soil. Sediment. 12, 542–555. https://doi.org/10.1007/s11368-011-0468-7.
Pierantoni, P.P., Penza, G., Macchiavelli, C., Schettino, A., Turco, E., 2020. Kinematics of the Tyrrhenian-Apennine system and implications for the origin of the Campanian magmatism. In: Vesuvius, Campi Flegrei, and Campanian Volcanism. Elsevier, pp. 33–56.
Pitcairn, I.K., 2011. Background concentrations of gold in different rock types. Appl. Earth Sci. 120 (1), 31–38. https://doi.org/10.1179/1743275811Y.0000000021.
Pokrovski, G.S., Borisova, A.Y., Roux, J., Hazemann, J.-L., Petdang, A., Tella, M., Testemale, D., 2006. Antimony speciation in saline hydrothermal fluids: a combined X-ray absorption fine structure spectroscopy and solubility study. Geochim. Cosmochim. Acta 70, 4196–4214.
Pollini, L., Bucelli, P., Calò, A., Costantini, E.A.C., L'Abate, G., Lorenzetti, R., Lisanti, M. T., Malorgio, G., Moio, L., Pomarici, E., Storchi, P., Tomasi, D., 2013. Atlante dei territori del vino italiano. Enoteca Italiana, Pacini Ed., Siena.
Raimondi, G., Di Stasio, E., Barbieri, G., Rouphael, Y., De Pascale, S., 2021. Nutritional and functional profiling of traditional Italian 'San Marzano' tomatoes. Acta Hortic. 1320, 65–70. https://doi.org/10.17660/ActaHortic.2021.1320.8.
Randall, G.W., Hoeft, R.G., 1988. Placement methods for improved efficiency of P and K fertilizers: a review. J. Prod. Agric. 1 (1), 70–79.
Rao, R., Corrado, G., Bianchi, M., Di Mauro, A., 2006. (GATA)$_4$ DNA fingerprinting identifies morphologically characterized 'San Marzano' tomato plants. Plant Breed. 125 (2), 173–176. https://doi.org/10.1111/j.1439-0523.2006.01183.x.
Rashid, A., Schutte, B.J., Ulery, A., Deyholos, M.K., Sanogo, S., Lehnhoff, E.A., Beck, L., 2023. Heavy metal contamination in agricultural soil: Environmental pollutants affecting crop health. Agronomy 13, 1521.
Reimann, C., Filzmoser, P., 2000. Normal and lognormal data distribution in geochemistry: death of a myth. Consequences for the statistical treatment of geochemical and environmental data. Environ. Geol. 39, 1001–1014. https://doi.org/10.1007/s002549900081.
Reimann, C., Filzmoser, P., Garrett, R.G., 2005. Background and threshold: critical comparison of methods of determination. Sci. Total Environ. 346 (1–3), 1–16.
Reimann, C., Filzmoser, P., Fabian, K., Hron, K., Birke, M., Demetriades, A., GEMAS Project Team, 2012. The concept of compositional data analysis in practice—Total major element concentrations in agricultural and grazing land soils of Europe. Sci. Total Environ. 426, 196–210.
Rollinson, H.R., 1993. Using geochemical data: evaluation, presentation, interpretation. Longman Group UK Ltd.
Roviello, V., Caruso, U., Dal Poggetto, G., Naviglio, D., 2021. Assessment of copper and heavy metals in family-run vineyard soils and wines of Campania region, South Italy. Int. J. Environ. Res. Public Health 18 (16), 8465. https://doi.org/10.3390/ijerph18168465.
Selin, N.E., 2009. Global biogeochemical cycling of mercury: a review. Annu. Rev. Environ. Resour. 34, 43–63.
SNPA, 2018. Linee guida per la determinazione dei valori di fondo per i suoli ed per le acque sotterranee. Linee Guida SNPA n. 8/2018 (Ex manuali e Linee Guida ISPRA 174/2018). ISPRA. ISBN 978-88-448-0880-8.
SNPA, Sistema Nazionale per la Protezione dell''Ambiente, 2023. Environmental Report: Italy. https://www.snpambiente.it/snpa/rapporto-ambiente-snpa-edizione-2023/ (in Italian).
Southworth, G., Lindberg, S., Zhang, H., Anscombe, F., 2004. Fugitive mercury emissions from a chlor-alkali factory: sources and fluxes to the atmosphere. Atmos. Environ. 38, 597–610.
Steckler, M.S., Agostinetti, N.P., Wilson, C.K., Roselli, P., Seeber, L., Amato, A., Lerner-Lam, A., 2008. Crustal structure in the southern Apennines from teleseismic receiver functions. Geology 36 (2), 155–158.
Tranchida-Lombardo, V., Aiese Cigliano, R., Anzar, I., Landi, S., Palombieri, S., Colantuono, C., Bostan, H., Termolino, P., Aversano, R., Batelli, G., et al., 2018. Whole-genome re-sequencing of two Italian tomato landraces reveals sequence variations in genes associated with stress tolerance, fruit quality, and long shelf-life traits. DNA Res. 25, 149–160. https://doi.org/10.1093/dnares/dsx045.
USEPA, 2022. ProUCL: statistical software for environmental applications for data sets with and without nondetect observations. Version 5.2. https://www.epa.gov/land-research/proucl-software.
Venables, W.N., Ripley, B.D., 2002. Modern applied statistics with S, 4th ed. Springer. https://doi.org/10.1007/978-0-387-21706-2.
Verdi, L., Mancini, M., Ljubojevic, M., Orlandini, S., Dalla Marta, A., 2018. Greenhouse gas and ammonia emissions from soil: the effect of organic matter and fertilisation method. Ital. J. Agron. 13 (3), 260–266.
Vitale, S., Ciarcia, S., 2018. Tectono-stratigraphic setting of the Campania region (southern Italy). J. Maps 14 (2), 9–21.
Wang, X.S., Qin, Y., 2006. Spatial distribution of metals in urban topsoils of Xuzhou (China): Controlling factors and environmental implications. Environ. Geol. 49, 905–914.
West, R.M., 2021. Best practice in statistics: use the Welch t-test when testing the difference between two groups. Ann. Clin. Biochem. 58 (4), 267–269. https://doi.org/10.1177/0004563221992088ces.
Wu, Y., Li, X., Gong, Q., Wu, X., Yao, N., Peng, C., Chao, Y., Wang, X., Pu, X., 2021. Test and application of the geochemical lithogene on weathering profiles developed over granitic and basaltic rocks in China. Appl. Geochem. 128, 104958. https://doi.org/10.1016/j.apgeochem.2021.104958.
Xia, X., Ji, J., Zhang, C., Huang, C., Lu, X., Yang, Z., 2024. The degree of soil arsenic background enrichment by carbonate weathering is mainly controlled by climate in large spatial scale. Sci. Total Environ. 951, 175868. https://doi.org/10.1016/j.scitotenv.2024.175868.
Yan, T., Wu, X., Quan, Y., Gong, Q., Li, X., Wang, P., Li, R., 2018. Heredity, inheritance, and similarity of element behaviors among parent rocks and their weathered products: a geochemical lithogene. Geoscience 32, 453–467 (In Chinese with English abstract).
Yan, G., Mao, L., Jiang, B., Chen, X., Gao, Y., Chen, C., Li, F., Chen, L., 2020. The source apportionment, pollution characteristic, and mobility of Sb in roadside soils affected by traffic and industrial activities. J. Hazard. Mater. 384, 121352.
Zuo, R., Wang, J., 2016. Fractal/multifractal modeling of geochemical data: a review. J. Geochem. Explor. 164, 33–41.
Zuzolo, D., Cicchella, D., Catani, V., et al., 2017. Assessment of potentially harmful element pollution in the Calore River basin (Southern Italy). Environ. Geochem. Health 39, 531–548. https://doi.org/10.1007/s10653-016-9832-2.
Zuzolo, D., Cicchella, D., Lima, A., Guagliardi, I., Cerino, P., Pizzolante, A., Thiombane, M., De Vivo, B., Albanese, S., 2020. Potentially toxic elements in soils of Campania region (Southern Italy): combining raw and compositional data. J. Geochem. Explor. 213, 106524. https://doi.org/10.1016/j.gexplo.2020.106524.